TEMPORAL-DIFFERENCING AND REGION-GROWING TECHNIQUES TO IMPROVE TWILIGHT LOW CLOUD DETECTION FROM SEVIRI DATA

Marcel Derrien, Hervé Le Gléau

Météo-France / DP / Centre de Météorologie Spatiale. BP 50747. 22307 Lannion. France

Abstract

The European Organization for the Exploitation of Meteorological Satellites (EUMETSAT), through the Satellite Application Facility in support to Nowcasting (SAFNWC) is aiming to provide a software package suitable to generate products derived from the Spinning Enhanced Visible and Infrared Imager (SEVIRI) onboard the METEOSAT Second Generation Satellite (MSG). A cloud mask is one of its key derived products. A visual analysis of its behaviour through animation loops indicates a discontinuity in the detection of low clouds in the vicinity of the day-night transition. Thus its use as input to other numerical processing may have a negative impact when the scene includes a day-night transition. The study described in this paper is aiming to produce a smoother continuity of the cloud mask. It is shown that a temporal-differencing technique combined with a region-growing technique can improve low level cloudiness detection in day-night transition area without increasing false alarms. The technique is described and the resulting improvement is illustrated. A preliminary comparison of statistics of the cloudiness over Europe reported in SYNOP and retrieved from SEVIRI with and without the enhancement estimates a decrease of 53% of the frequency of non detected clouds with a weak increase of false alarm ratio, giving now better results than night-time method.

BACKGROUND

The Satellite Application Facility in support to Nowcasting (SAFNWC) is part of EUMETSAT ground segment (Schmetz et al. 2002). It provides targeted users with software packages for the generation of satellite-derived products useful for nowcasting purposes. One package is designed specifically for data on board polar platform satellites (NOAA and METOP) and the other one for the data of geostationary satellite Meteosat Second Generation (MSG). Here we focus on a study designed for the geostationary SAFNWC/MSG package whose first operational release has been distributed to users since June 2004.

The SAFNWC/MSG cloud mask (CMa) and cloud type (CT) algorithms have been developed by the Centre de Météorologie Spatiale (CMS) of Météo-France (Derrien and Le Gléau, 2005). They are based on a thresholding technique. The thresholds are adapted to the atmosphere and surface conditions, forecasted by a Numerical Weather Prediction (NWP) model or derived from climatologies when NWP data are not available, and the sun–satellite viewing geometry using cloud-free radiative transfer model simulations. Static or dynamic, spectral and textural features are used and the sequence of employed tests depends upon the earth surface and the sun-satellite geometry, but this first design does not exploit the temporal information content of geostationary imagery.

Around sunrise and sunset it is frequent to observe low clouds disappearing and reappearing in SAFNWC/MSG cloud mask time series. That shows up that such clouds are often undetected over day-night transition areas. This major shortcoming has been reported by Météo-France forecasters using CT to analyse cloud cover, especially around sunrise when low level cloudiness is increased by high moisture concentration in low atmosphere while ground-based observations may be sparse and satellite imagery the only tool for its estimation. A solution to this problem was also claimed in the conclusions of a SAFNWC users workshop held at Madrid in 2005. V. Guidard and D. Tzanos, 2007,

use CT provided by SAFNWC/MSG combined with ground measurements and a hourly surface analysis as input to their automatic analysis of fog probability over land to estimate where fog is likely to occur. They ascribe most of their non-detections to bad cloud mask in twilight conditions. CT from the SAFNWC/MSG is also used in a Météo-France 3D-Var data assimilation system to select SEVIRI radiances not contaminated by clouds (Montmerle, 2005). Of course this assimilation system is also sensitive to low cloud misses during periods of twilight.

This poor result near day-night terminator is a consequence of the difficulty of simulation of the behaviour of the bidirectional reflectance factor (BRF) when sunlight decreases and a lack of simulation of the solar component within the short wave 3.9μm measured radiance around day-night transition. Therefore thresholds that are computed for SAFNWC/MSG algorithm become inefficient. When examining an enhanced VIS image one can rather easily distinguish low clouds that are not automatically detected in the cloud mask, so that it is clear that some information remains unexploited here.

Cloud missing near day-night terminator is not specific to SAFNWC/MSG cloud mask and several authors have reported this matter and sometimes proposed improvements. Lee et al, 1997, replace the ambiguous pixels along the terminator by those from a previous image to provide forecasters with around-the-clock red-green-blue composite images. Trepte et al, 2005, improve their twilight cloud and snow detection using GOES-9 data by improving and giving more weight to their reflectance thresholds in low sun conditions. d'Entremont and Gustafson, 2006, introduce an empirical solar adjustment function to normalize Visible BRF before comparison with clear-sky values from a dynamic database obtained from previous observations. This adjustment is aimed to improve their detection in twilight conditions.

APPROACH

In the SAFNWC/MSG cloud mask, low clouds are rather well detected at night (T10.8-T3.9 or T10.8-T8.7) and even better at daytime (VIS (at 0.6μm or 0.8μm), 3.9μm reflectance). They disappear only during the periods of twilight. Low clouds generally move slowly, and their thermal characteristics are almost invariant within one hour. Moreover when stratiform, they often present a uniform and flat deck, with a locally homogeneous reflectance. For these reasons, we have studied a first technique using the persistent characteristics of such clouds to improve their detection around day-night terminator, driven by the same idea as Lee et al, 1997, for their colour composite image improvement.

Classically the temporal-differencing technique, i.e. the calculation of difference of features observed at two different times, is employed to identify pixels whose spectral characteristics have changed with time in order to declare them as cloudy. Therefore, used in such a way, it is efficient for detection of rapidly developing or moving cloud features. The registration quality of the involved images must be good as any registration error in one image may lead to anomalous cloud signatures. Here we use temporal-differencing in an opposite way. First we search inside the day-night transition portion of the current image pixels that were previously detected as low clouds and keep their radiometric attributes. If they remain identical in the current image we restore them as cloudy. This approach is suited to detect persistent and stationary cloud features only. Obviously the quality of the result relies mainly on the quality of the previous cloud mask. Therefore, to avoid false alarms, strict constraints must be set when selecting the stationary cloud pixels in the previous image. A registration error in one image may lead to cloud missing but should be less critical concerning false alarms.

When analysing the results obtained by this first step during testing, we were not fully satisfied because cloud parts remained undetected, but still discernible in enhanced VIS image. In general the inner part of low cloud decks were caught while their optically thinner part or new portions appearing with the cloud development or its forward motion may have passed through the temporal differencing procedure and kept as clear.

To improve the detection of the outer part of the cloud we decided to use the radiometric statistical attributes of the newly detected pixels as constraints of a region-growing technique applied to the initial stationary pixels identified by the first step. The goal of this second step is to spatially extend the

initial cloud “seeds” to their connected pixels presenting similar characteristics. Such a process may also lead to false alarms if constraints are too loose.

After these two steps it may happen that some moving or growing low cloud decks remain undetected. A supplementary time-differencing step as used by d’Entremont and Gustafson, 2003, searches among the remaining clear pixels in the current image those whose spectral characteristics have changed with time to declare them as cloudy. This last step is applied to the whole image, including or not the day-night terminator area. It is more efficient for detection of high thin clouds moving rapidly but may also catch the growing part of a low cloud colder than its underlying surface. As not specific to the day-night transition it will not be described here for clarity purposes.

ALGORITHM DESCRIPTION

Temporal-differencing for stationary low clouds detection in day-night transition area.

The day-night terminator separates sunlit from dark regions and its line is apparent near local sunrise and sunset. It crosses the earth's disk with a speed about 1600 km/h in equatorial regions. Its orientation varies with the season, showing a larger sunlit area in the higher latitudes during summer. If defining the day-night transition as the area where sun zenith angle θ is between 80° and 93°, about one hour is necessary to get separated zones near equator, for high latitude regions it may be longer. Therefore a one-hour time interval between images is a minimum if one wants to get a given “twilight” pixel previously analysed by the day or night algorithm.

First, the SAFNWC/MSG Cloud Mask algorithm is applied as primary cloud detection for the current image. Its day-night transition portion is delimited according to sun zenith angle, and temporal differences of features that are known nearly insensitive to solar illumination change for a low cloud target are computed: $|\Delta_{1h}(T10.8)|$, $|\Delta_{1h}(T10.8\text{-}T12.0)|$, $|\Delta_{1h}(T10.8\text{-}T8.7)|$ where $|\Delta_{1h}|$ is the absolute value of temporal difference with a time interval of one hour. The CMa_{1h} and CT_{1h} of the previous image are used to identify pixels previously classified as low or medium clouds one hour earlier and detected by a high confidence test. Those pixels are restored as cloudy in the current transition area if the absolute values of temporal features, noted Δ_{1h},satisfy the following conditions:

over land $|\Delta_{1h}(T10.8)| < 1.0K$, and $|\Delta_{1h}(T10.8\text{-}T8.7)| < 0.5K$

over water $|\Delta_{1h}(T10.8)| < 1.0K$ and $|\Delta_{1h}(T10.8\text{-}T12.0)| < 0.6K$

Typical false alarms brought by this step are induced by those of the method applied one hour sooner because a clear pixel mistakenly classified as cloud would generally satisfy the tests.

Region-growing for spatial expansion of initial low cloud patches

To account for variations in solar illumination when computing TOA BRF a very popular normalization used when screening VIS images is an inverse cosine function of θ. This purely geometric normalization is an air-mass correction of the solar beam pathlength assuming atmosphere is plane parallel. In day-night terminator area this assumption is no longer correct, and two effects become important: curvature of atmosphere and refraction. When sun zenith angle approaches 90°, because of curvature of atmosphere the solar beam pathlength is significantly shorter than the plane parallel one. This explains why for VIS pictures normalized using this inverse cosine function, VIS values displayed near day-night terminator appear too high.

Twilight whose exact definition is the diffused light in the sky when the sun is just below the horizon, just after sunset or just before sunrise, is an effect of atmospheric refraction. The refractive index of air decreases when wavelength increases, in other words, blue light, which comprises the shortest wavelength region in visible light, is refracted at significantly greater angles than is red light. Refraction may be neglected even for θ near 85°, but not when caring about features in rather low atmosphere for higher θ.

For these two reasons we have replaced the inverse cosine BRF normalization function by an analytical formulation valid for a standard atmosphere proposed by Li and Shibata, 2006. Their parameterization accounts for spherical atmosphere and refraction, and it has been preferred to older

expressions proposed by Kasten,1966 and Rodgers,1967 that have been shown overestimating the normalization factor. Aware that this parameterization should be adapted to the narrowband spectral characteristics of each VIS band of SEVIRI and to the current state of atmosphere, we keep it as a first order correction for a better handling of VIS BRF in twilight area. Figure 1 compares it with inverse cosine normalization.

Short wavelengths are more sensitive to Rayleigh and aerosol scattering (haze, smoke, dust, pollen…), therefore the contrast between low clouds and atmosphere improves noticeably as wavelength increases. But near-infrared cloud-free reflectance over land is usually much higher than at shorter wavelengths therefore contrast reduces between low clouds and bright grounds at this wavelength. Considering that low clouds are our main target around day-night terminator, we have decided to use VIS06 channel to improve detection at twilight for any underlying surface condition.

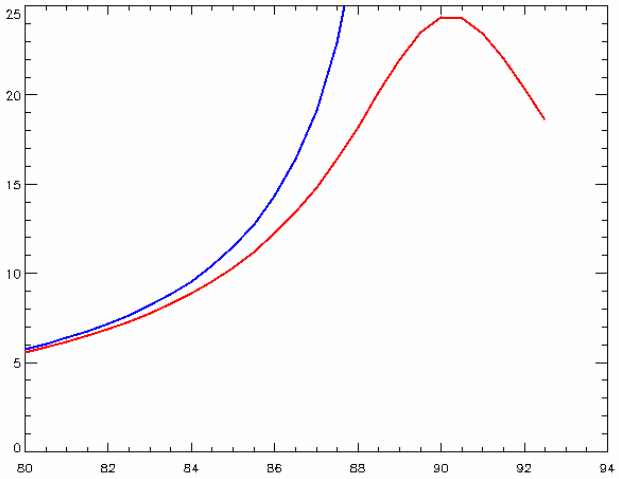

Figure 1: **Comparison of VIS normalization factor variation with sun zenith angle, inverse cosine (blue) and parameterization given by Li et al 2006 (red)**

Because BRF of pixels in day-night terminator portion becomes very sensitive to noise when approaching the terminator line, we allow region-growing for $75° < \theta < 89°$. Groups of connected pixels restored by the first temporal-differencing method form initial seeds for the region-growing are identified. Any group comprising more than eight elements is taken into account. For each significant group two mean values are computed: normalized BRF0.6 (AVG0.6) and T108 (AVG10.8). A group is expanded while a 8-connectivity neighbour pixel x belonging to the day-night transition area satisfies simultaneously the following conditions:

$SCAT_x < 150°$

$BRF0.6_x > MAX(1.05*AVG0.6, THR_{exp})$

$AVG10.8 + 0.5K < T10.8_x < AVG10.8 - 5.0K$

Where THR_{exp} is 40% over Africa to avoid false alarms over arid areas and 30% elsewhere

$SCAT_x$ is the scattering angle [0°,180°], 0° for backward scattering

$BRF0.6_x$ is the normalized BRF in VIS06 SEVIRI at location x

$T10.8_x$ is the brightness temperature of SEVIRI 10.8 μm at location x

The main risk of the method is to add cloud false alarms and it is maximal when the radiometer is looking in the sun direction because measured clear-sky BRF0.6 increase dramatically. That is why we forbid region growing at locations where scattering angle is greater than 150°. Moreover we reject region-growing restoring more than 10000 elements for the same seed assuming that a too wide region-growing is suspect. The strategy employed in the region-growing technique may produce small differences in presence of blurry low cloud edges resulting in small jumps in cloud features animations.

A cloud becoming optically thinner or a high cloud placed in the direction of the sun and casting a long shadow (emphasized by low sun elevation) over a low cloud deck or a shady cloud slope, may escape this test because its too low BRF. If not caught by some night tests and sometimes still efficient (T10.8-T3.9, T10.8-T8.7) such pixels may remain undetected after the region-growing step.

EXAMPLES

The algorithm described above is running in checkout mode at Météo-France since 17 July 2007 and its results are being analysed by targeted forecasters. The examples given in this section have been gathered from this production set and therefore are limited to summer cases.

Sunrise example

Figure 1 illustrates the efficiency of the algorithm to restore wide missed parts of an extensive area of low cloud over northern France and United Kingdom moving in a NW advection. Some outer edge parts remaining undetected in areas of clouds presenting more ragged shapes are observable on the right image.

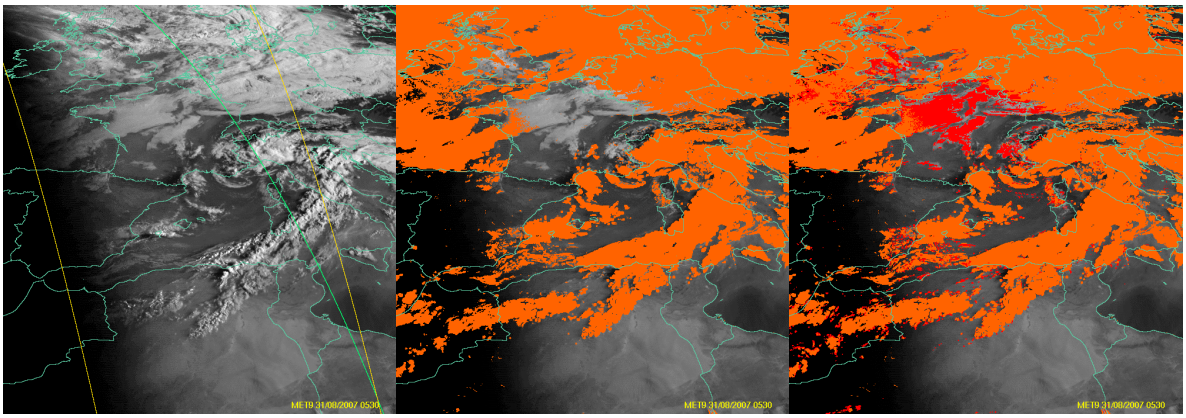

Figure 2: **31 August 2007, 05h30 UTC METEOSAT 9 left: Normalized SEVIRI 0.6 with limits of transition area (yellow) and 1h sooner (green) centre: SAFNWC/MSG v2.0 cloud mask (orange) superimposed with SEVIRI 0.6 right: same as centre with new twilight detection (red).**

Sunset example

This case illustrates how the new scheme handles a weakness of SAFNWC/MSG v2.0 to detect a barrage cloud formed in the windward side of Pyrénées in France and Cantabrica in Spain. As such clouds are rather immobile during the one-hour interval, they are more easily detected and their pattern is better restored than for patchy Sc as in previous example.

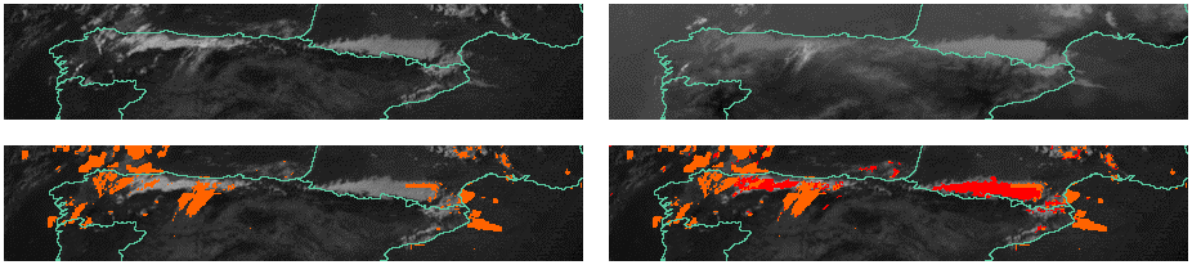

Figure 3: **24 July 2007, 18h45 UTC METEOSAT 9 top left: Normalized SEVIRI 0.6 top right: enhanced SEVIRI 10.8 bottom left: SAFNWC/MSG v2.0 cloud mask (orange) superimposed with SEVIRI 0.6 bottom right: SAFNWC/MSG v2.0 cloud mask (orange) and new twilight detection (red) superimposed with SEVIRI 0.6**

VALIDATION

A validation dataset merging European SYNOP data, SAFNWC/MSG v2.0 cloud masks without and with the cloud detection by the new twilight scheme, has been settled. Data from 1 August 2007 till 9 September 2007 have been used for this preliminary analysis. Ground-based total cloud coverage (N) is available in SYNOP data. Satellite-based cloudiness is estimated from 5x5 boxes of cloud mask

centred on the SYNOP location by counting cloud contaminated pixels as fully cloud covered. This match-up database is used to assess the new "twilight scheme".

A situation is classified as clear when total coverage N $\leq$2 and cloudy when N $\geq$6. Contingency tables as presented in Table 1 are used to compute statistical indicators; percentage of correct results (PC=(h+cr)/(h+cm+fa+cr), cloud miss rate (MR=m/(h+m)) and false alarm ratio, (FAR=fa/(h+fa)). The results for situations stratified by their detection method (day (sun zenith angle lower than 80°), night (sun zenith angle larger than 93°), twilight v2.0 and new twilight scheme) are given in table 2 and their statistics in table 3.

	Detected cloudy	**Detected clear**
Observed cloudy	h	m
Observed clear	fa	cr

Table 1: **Contingency tables convention, clear when total coverage N ≤2 and cloudy when N ≥6, h for hits, m for misses, fa for false alarms, cr for correct rejections**.

	h	**m**	**fa**	**cr**	**Total**
Day v2.0	53212	1076	1243	29085	84616
Night v2.0	21373	1822	2281	25164	50640
Twilight v2.0	11250	1560	286	7741	20837
New twilight scheme	12237	732	361	8294	20892

Table 2: **Contingency tables stratified by detection methods with h,m,fa and cr defined in Table 1.**

This limited dataset clearly shows that the new scheme greatly improves the cloud detection in twilight condition, as the frequency of non detection (MR) decreases by 53%, while the FAR increase is only 16%. Moreover, the "new twilight" cloud detection's quality is better than the one achieved at night-time as all its indicators are better. Of course these preliminary conclusions should be confirmed by an analysis on a longer time period.

	PC	**MR**	**FAR**
Day v2.0	97.3%	2.0%	2.3%
Night v2.0	91.9%	7.9%	9.6%
Twilight v2.0	91.1%	12.2%	2.5%
New twilight scheme	94.8%	5.6%	2.9%

Table 3: **Statistical scores stratified by detection methods, PC, MR and FAR defined in text.**

CONCLUSION

This paper describes a new technique designed to detect cloudiness by low clouds around day-night transition which is shown to greatly improve cloud detection indicators. SAFNWC/MSG v2.0 is its primary cloud detector. The improved scheme makes also use of previous cloud mask and type and SEVIRI data obtained one hour sooner to restore cloud seeds presenting stationary characteristics with time in several SEVIRI infra-red bands. Normalization of VIS information has been reconsidered to make these reflectances useful to restore missed clouds by a region-growing technique starting from cloud seeds. This new scheme was estimated mature enough to be experimented in checkout mode at Météo-France since 17 July 2007. Its results are being analysed by targeted forecasters before an operational implementation. After a longer operational experimentation at Météo-France it will be proposed to be embedded in SAFNWC/MSG package.

AKNOWLEDGEMENTS

The authors are grateful to the IPL98 developers for making available their library as a free software distributed under GNU licence and downloadable at URL http://www.mip.sdu.dk/ipl98.

REFERENCES

d'Entremont R. and Gustafson G., 2003: Analysis of Geostationary Satellite Imagery Using a Temporal-Differencing Technique, Earth Interactions.

d'Entremont R. and Gustafson G., 2006: Cloud Detection and Property Retrieval Across The Day/night Terminator. 14th Conference on Satellite Meteorology and Oceanography.

Derrien M. and Le Gléau H., 2005: MSG/SEVIRI Cloud Mask and Type from SAFNWC, I.J.R.S., vol. **26**, No. 21, pp 4707–4732, DOI: 10.1080/01431160500166128

Guidard V. and Tzanos D., 2007: Analysis of Fog Probability from a Combination of Satellite and Ground Observation Data, Pure Appl. Geophys., DOI: 10.1007/s00024-007-0215-6

Kasten K., 1966: A new table and approximate formula for relative optical air-mass. Arch. Meteor. Geophys. Bioklimatol. Ser. B, **14**, pp 206-233.

Lee T. F., Turk F. J., and Richardson K., 1997, Stratus and Fog Products using GOES-8 3.9μm Data, Weather and Forecasting, **12**, pp 664-667.

Li J. and Shibata K., 2006, On the effective solar pathlength, J.A.S., Vol **63**, Issue 4, pp 1365-1373

Montmerle T., 2005, Impact of SEVIRI IR radiances in Météo-France's operational 3D-Var assimilation system at regional scale. The 2005 EUMETSAT Meteorological Satellite Conference, Dubrovnik, Croatia, 19-23 September 2005. EUMETSAT P.46, ISBN 92-9110-073-0

Rodgers C., 1967: The radiative heat budget of the troposphere and lower stratosphere. Planetary Circulation Project, Department of Meteorology, Rep. A2, Massachusetts Institute of Technology.

Schmetz J., Pili P., Tjemkes S., Just D., Kerkmann J., Rota S., and Ratier A., 2002: An Introduction to Meteosat Second Generation (MSG). Bull. Amer. Meteor. Soc., **83**, pp 977–992.

Trepte, Q.Z., Minnis P., and Palikonda M., 2005: Improvements in near-terminator and nocturnal cloud masks using satellite imager data over the ARM sites. Proceedings of the Fifteenth ARM Science Team Meeting, Daytona Beach, Florida, March 14-18.